Inorganica Chimica Acta, 62 (1982) 171–182

The Photoelectron Spectra of Bis(cyclopentadienyl)titanium Derivatives – a Green's Function Approach

MICHAEL C. BÖHM

Organisch-Chemisches Institut der Universität, Im Neuenheimer Feld 270, D69 Heidelberg, F.R.G.

Received January 28, 1982

The low energy photoelectron spectra of bis-(cyclopentadienyl)titaniumdicarbonyl (1) and of the dihalide complexes with F (2), Cl (3) and Br (4) have been studied by means of semiempirical MO calculations of the CNDO/INDO type in the framework of many-body perturbation theory, based on the Green's function formalism. The theoretically-determined ionization energies are compared with available experimental data. It is shown that the electronic structure of the dihalide complexes 2–4 can be rationalized on the basis of a MO model that takes into account the interaction strength between the cyclopentadienyl π orbitals and the halide lone-pair and σ combinations. The measured vertical ionization potentials are reproduced satisfactorily by the theoretical approach. In contrast to previous experience in the transition metal field it is demonstrated that Koopmans' theorem is a sufficient approximation for the assignment of the outer valence ionization events. These findings for the Ti complexes are compared with calculated re-organization energies in 3d complexes with Fe, Co or Ni as the transition metal center.

Introduction

The chemistry of bent bis(π-cyclopentadienyl) complexes with Ti, Zr and Hf as the central atom has found enlarged interest in recent years [1]. These systems often show catalytic activities in various insertion reactions of coordinated olefins [2]. Consequently, the electronic structure of bent sandwich complexes has been the subject of a series of theoretical investigations. A qualitative MO model was developed by Ballhausen and Dahl [3], which has been modified by Alcock [4] and by Green and co-workers [5]. The validity of these qualitative models has been analyzed in the computational framework of one-electron approaches of the Wolfsberg-Helmholtz or the Extended Hückel (EH) type [6, 7]. On the other hand several studies on the photoelectron (PE) spectra of bis(cyclopentadienyl) transition metal derivatives have been published where a feedback to theoretical models for the assignment of the measured ionization potentials was not realized. Fragalá and co-workers have investigated the He(I) and He(II) PE spectra of bis(cyclopentadienyl)titanumdicarbonyl [8]. The He(I) and He(II) spectra of different bis(cyclopentadienyl)metal dihalides in the outer valence region have been published by various groups [9–12]. The PE data of the Ti derivatives with fluorine and bromine were presented without computational results; divergent assignments based on the validity of Koopmans' theorem [13] ($I_{v,j} = -\epsilon_j$) have been reported for the corresponding chlorine derivative [9, 10].

Therefore we have analyzed the electronic structure of some bent Ti complexes within an improved CNDO/INDO extension to the 3d series [14], and assigned their PE spectra in the lower energy region by means of theoretical methods that are beyond Koopmans' theorem [13] and beyond the well-known ΔSCF approximation where only the relaxation contributions of the total electronic reorganization are considered [15]. To take into account relaxation and correlation effects accompanying the ionization events we have determined the vertical ionization potentials (IPs) in the framework of the one-particle Green's function formalism [16].

In the present study we have analyzed the outer valence region in the PE spectra of bis(π-cyclopentadienyl)titanumdicarbonyl (*1*) and of the bis(π-cyclopentadienyl)titanum dihalides with F (*2*), Cl (*3*) and Br (*4*), by means of a perturbational approach based on the Green's function method.

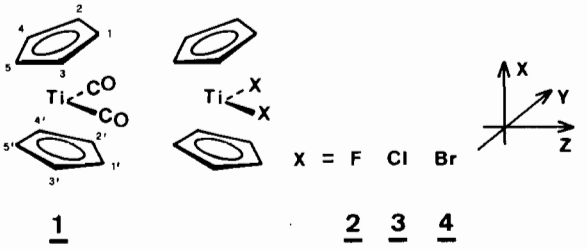

1 **2** **3** **4**

0020-1693/82/0000-0000/$02.75

Computational Aspects

The determination of the vertical ionization energies *via* the one-particle Green's function requires the determination of those ω values for which the matrix of the inverse Dyson equation [17] has eigenvalues equal to zero:

$$G^{-1} = (G^{\circ})^{-1} - \Sigma(\omega) = \omega I - \epsilon - \Sigma(\omega)$$

In the above formula G symbolizes the matrix of the Green's function and G° the corresponding matrix of the free Green's function which is related to the canonical Hartree-Fock orbitals and the one-electron energies ϵ that diagonalize the Fock operator. Therefore $(G^{\circ})^{-1}$ is given by $(\omega I - \epsilon)$, where I stands for the unit matrix of proper size. $\Sigma(\omega)$ symbolizes the self-energy operator which must be expanded into a perturbational series. If canonical HF orbitals are used as zero order approximations, $\Sigma^{(1)}(\omega)$ vanishes and the expansion of $\Sigma(\omega)$ starts with second order terms [16, 18].

$$\Sigma(\omega) = \Sigma^{(2)}(\omega) + \Sigma^{(3)}(\omega) + \cdots + \Sigma^{(\infty)}(\omega)$$

Generally the convergence of this perturbational series is rather slow. A sufficient approximation to $\Sigma(\omega)$ can thus be expected if higher order contributions to the self-energy operator are taken into account, by means of a re-normalized model potential. Cederbaum [19] has derived an $\Sigma(\omega)$ expression based on Kelly's geometrical approximation [20]. In this model only a single third order increment must be added to $\Sigma^{(2)}(\omega)$ to construct a renormalized ansatz $\Sigma^{\mathrm{eff}}(\omega)$ for the self-energy expansion.

$$\Sigma^{\mathrm{eff}}(\omega) = \Sigma^{(2)}(\omega) + D4$$

The explicit expressions for the self-energy elements can be found in the literature [16, 19]; the decomposition of the re-normalized model potential into relaxation and correlation parameters has been described elsewhere [21]. In the framework of our semiempirical CNDO/INDO Hamiltonian this effective approximation has been used with remarkable success for the determination of vertical ionization potentials of organometallics in the outer valence region [22].

For the determination of the energy parameter ω we have used simplifications that are part of most Green's function calculations, by means of semiempirical MO models [23]. Thus $\Sigma(\omega)$ is assumed to be diagonal [24].

$$\Sigma_{ij}(\omega) = \Sigma_{ij}(\omega)\delta_{ij}$$

In the second order elements of the self-energy part a Taylor series expansion about the main pole (Koopmans' pole) is performed [25], while ω_j in the third order contribution is substituted by ϵ_j, which corresponds to a Rayleigh-Schrödinger approximation to the perturbational expansion.

All MO calculations on *1–4* were performed with a recently-designed CNDO/INDO model for elements up to bromine [14]. In the case of *1*, *2* and *3* the INDO approximation of the semiempirical all-valence procedure has been used; the one-center exchange integrals are given in terms of experimentally-derived Slater-Condon parameters [14]. In the case of the Br complex *4*, no exchange parameters are available for the halide center. Therefore the CNDO form of our model Hamiltonian has been used for the Br compound. The electron core interaction integrals were determined by means of Pople's original CNDO/2 approximation [26], penetration effects being neglected.

For the calculations on *1–4* we have used geometrical parameters, determined either by X-ray investigations on the model systems or on studies of related species. In the case of *1* we have employed the bond lengths of Atwood and coworkers [27]: $TiC_{carbonyl}$ = 2.03 Å and an averaged $TiC_{cyclopentadienyl}$ value of 2.35 Å. The angle centroid(Cp)–Ti–centroid(Cp) is 138.6°, and the angle between Ti and the carbonyl groups is 87.9°. For the Cl complex *3* we have used the following values [28]: TiCl = 2.36 Å, $TiC_{cyclopentadienyl}$ = 2.32 Å while the two characteristic angles are 131° and 93.7° for the Cl–Ti–Cl fragment. As the exact structural parameters of *2* and *4* are not known, TiX distances from other titanum halides have been accepted (TiF = 2.13 Å [29], TiBr = 2.50 Å [30]). The remaining distances and bond angles in *2* and *4* were selected in accordance with the Cl derivative. In all complexes an eclipsed conformation of the cyclopentadienyl rings has been assumed, with a CC distance of 1.40 Å; for the CH bonds 1.10 Å have been accepted.

Ground State Properties of the Ti Complexes

In Table I we have summarized the orbital energies and the composition of the orbital wave function for the ten highest occupied orbitals of the dicarbonyl derivative *1*. In Fig. 1 a graphical representation of the five highest MOs is given. Formally, *1* can be considered as d^2 complex. As shown in Table I the HOMO of the Ti metallocene corresponds to this doubly occupied Ti 3d function. The Ti 3d character of the MO amounts to 52%, while 33% (Cp(π) contributions and 15% π^* admixtures from the CO groups are predicted. The Ti 3d amplitude is largest in the direction of the y-axis and thus can be classified as $3d_{y^2}$ AO. The complex HOMO corresponds to the $1a_1$ combination in the nomenclature of Lauher

TABLE I. Valence Orbitals of Bis(cyclopentadienyl)titanumdicarbonyl (*1*) According to an INDO Calculation. The Orbital Energies (ϵ_i) are Given in eV. The Composition (%), as well as the Irreducible Representation of the MO Wave Function, are indicated.

MO	Γ_i	MO-type	ϵ_i	% Ti	% Cp	% CO
37	$13a_1$	Ti $3d_{y^2}$	−8.07	51.8	33.1	15.1
36	$9b_1$	Cp(π), Ti $3d_{xz}$	−10.11	17.0	82.3	0.7
35	$9b_2$	Cp(π), Ti $3d_{yz}$	−10.45	9.9	89.7	0.4
34	$6a_2$	Cp(π), Ti $3d_{xy}$	−11.08	16.1	83.9	
33	$12a_1$	Cp(π), Ti $3d_{x^2-z^2}$	−11.36	15.7	84.1	0.2
32	$8b_1$	Cp(π)	−12.69	0.1	91.8	8.1
31	$8b_2$	Cp(σ)	−13.10	0.1	96.6	3.3
30	$11a_1$	Cp(σ)	−13.36	3.0	88.7	8.3
29	$5a_2$	Cp(σ), Ti $3d_{xy}$	−13.47	9.1	87.2	3.7
28	$7b_1$	Cp(σ), Ti $3d_{xz}$	−13.71	9.1	68.8	22.7

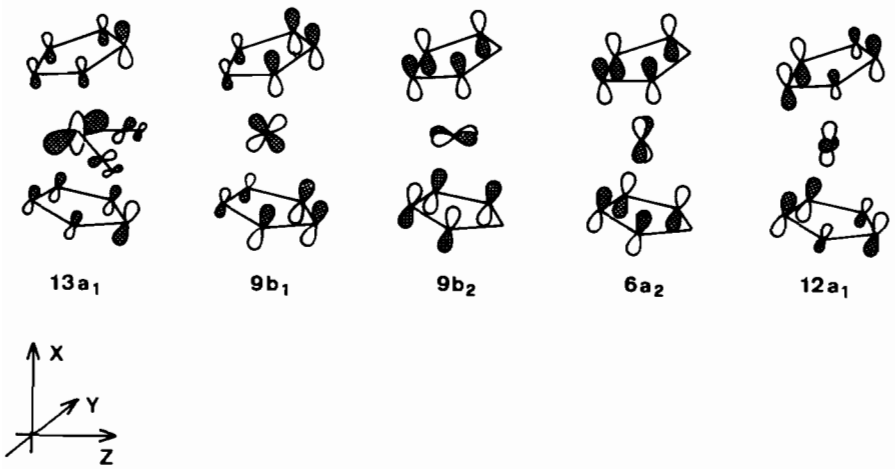

Fig. 1. Schematic representation of the five highest occupied MO's of bis(cyclopentadienyl)titaniumdicarbonyl.

and Hoffmann [7]. Figure 1 clearly shows that the Ti 3d function is stabilized by π^* of the CO ligands and also interacts in-phase with the Cp π orbitals. This MO is separated by about 2 eV from four orbitals with predominant Cp π character: $9b_1$, $9b_2$, $6a_2$ and $12a_1$ (the irreducible representations are labeled with respect to the valence electron configuration). These four MOs between −10.11 eV and −11.36 eV are related to the two degenerate Cp π combinations e_1'' and e_1' of an eclipsed metallocene [31]. $9b_1$ is a member of the e_1'' parent and contains significant Ti $3d_{xz}$ contributions. The Ti 3d AO interacts in-phase with the carbon centers of the Cp rings. $9b_2$ is derived from the e_1' set of an unperturbed metallocene. In contrast to $9b_1$, different phase relations between the central atom and the five-membered ligands are encountered. An antibonding interaction between Ti $3d_{yz}$ and C_2/C_3 and C_2'/C_3' respectively is predicted, while an in-phase relation in the case of the remaining C-centers (C_4/C_5 and C_4'/C_5') is diagnosed. Therefore different TiC bond-orders to the C atoms of the Cp ligands must be expected. $6a_2$ is the second member of the e_1'' set; the Cp π functions are stabilized by the Ti $3d_{xy}$ acceptor. $12a_1$ contains Ti 3d contributions that are bonding with respect to $C_1/C_4/C_5$ and $C_1'/C_4'/C_5'$, but destabilizing with respect to C_2/C_3 and C_2'/C_3'. The Ti 3d amplitude in these four MOs varies between 10 and 17%.

The remaining high-lying orbitals of *1* are separated by about 1.30 eV from $12a_1$ and are related to the a_2'' π combination of an eclipsed metallocene and to σ orbitals of the cyclopentadienyl fragments. At still lower energies the MO's of the CO ligands are found.

The MO schemes of *2–4*, which are formal d^0 complexes, are discussed under a common aspect. The high lying valence orbitals of the Ti derivatives *2* to *4* can be constructed from four fragment MO's localized at the Cp····Cp unit which are related to

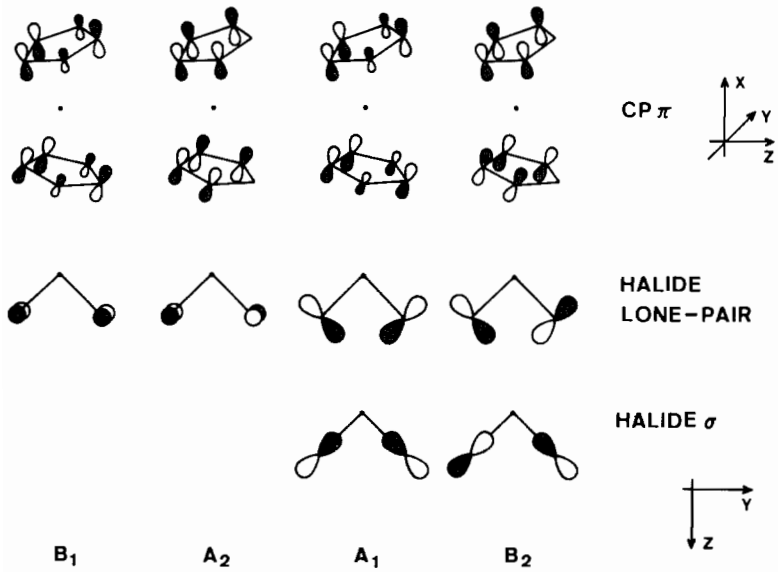

Fig. 2. Fragment orbitals of the Cp units (derived from e_1''/e_1' of an eclipsed metallocene) and the halide lone-pair and σ orbitals in the Ti derivatives *2–4*. The Ti 3d contributions have been omitted.

e_1'' and e_1' of the unbent metallocene. As already discussed in the case of the dicarbonyl complex those MO's transform under C_{2v} symmetry according to the irreducible representations B_1 and A_2 (e_1'' descendants), as well as according to B_2/A_1 (e_1' descendants). Next we have to consider the fragment orbitals of the XTiX moiety, the halide lone-pair combinations and the TiX σ functions. In Fig. 2 it is displayed that the lone-pair set gives rise to linear combinations of B_1, B_2, A_2 and A_1 symmetry, while the two TiX σ combinations transform according to A_1 and B_2 under C_{2v} symmetry. The MO's of *2–4* in the lower energy region therefore can be considered as linear combinations between the Cp π set derived from e_1'' and e_1', as well as from the six fragment orbitals localized at the XTiX fragment.

According to Cauletti *et al.* [12], three different coupling schemes can be distinguished as limiting cases of the interaction between both fragments (see Fig. 3). *A* describes the situation where the basis energies of the ligand π functions are placed significantly above the basis energies in the halide fragment. Due to a pronounced energy gap between both fragment orbitals, the coupling between the two moieties is weak and the four topmost orbitals of the dihalide complex are predominantly of the Cp π type, with small antibonding X conbributions. From these orbitals six MO's are separated where the MO wave functions contain predominant halide lone-pair or TiX σ character. In this set small bonding Cp π admixtures are found. In the case of *B* the basis energies of both fragments match each other and an ensemble of complex MOs must be expected, where comparable AO contributions from the formal subunits are encountered. The complex MO's therefore cannot be classified as Cp-type or halide-type orbitals as both moieties have lost their identity, due to the strong coupling. *C* corresponds to the situation where the halide fragment orbitals are found on top of the cyclopentadienyl combinations. With enlarged energy gaps between both basis orbitals reduced interactions between Cp and XTiX are found. In the case of weak coupling the dihalide complex is characterized by a set of six high-lying MOs with predominant X character, followed by four orbitals related to the Cp ligands (B_1, B_2, A_2 and A_1 symmetry). Between these limiting cases (*A*, *B* and *C*) a broad spectrum of interaction patterns is possible. In systems of class *A/B* with variable coupling strengths between the two fragments, outer valence orbitals with larger Cp π contributions are found; in the lower MOs a predominance of the halide amplitudes is expected. The opposite is true in complexes belonging to the bonding scheme *B/C*.

In Tables II–IV we have collected the INDO (*2*, *3*) and CNDO (*4*) results for the three dihalide complexes. It is recognized that the aforementioned classification is a suitable tool to rationalize the electronic structure of the Ti complexes. The fluorine system clearly belongs to class *A*. The four highest occupied MOs ($9b_1$, $8b_2$, $6a_2$ and $11a_1$) are predominantly of the Cp π type with F admixtures not exceeding 15%. The Ti 3d amplitudes in this MO family between −10.63 eV and −11.96 eV spans a range between 4% and 17%. Also the following MO ($8b_1$) is of Cp π character (a_2'' descendant). The four MOs with predominant F lone-pair contributions

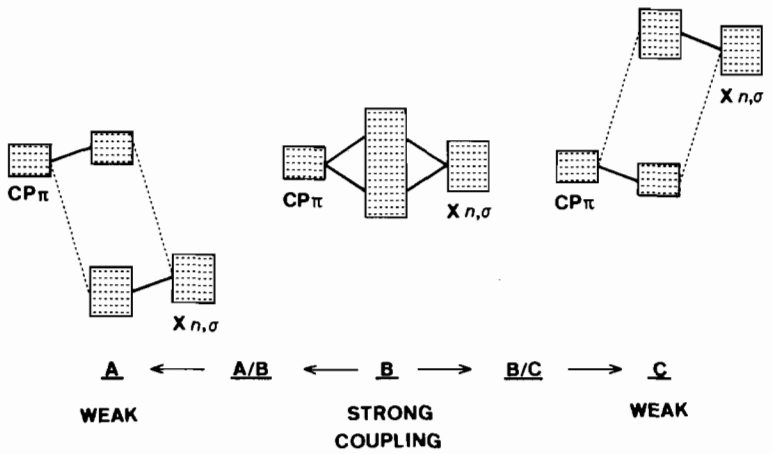

Fig. 3. Coupling schemes for the Cpπ and halide lone-pair and halide σ orbitals in the bent dihalide metallocenes. *A* and *C* correspond to the weak coupling limit between both fragments; in *B*, complex orbitals are encountered which contain comparable contributions from both fragments. *A/B* and *B/C* describe intermediate coupling schemes between the formal fragments.

TABLE II. Valence Orbitals of Bis(cyclopentadienyl)titanumdifluoride (*2*) According to an INDO Calculation. See Legend to Table I.

MO	Γ_i	MO-type	ϵ_i	% Ti	% Cp	% F
34	$9b_1$	Cp(π), Ti3d_{xz}	−10.63	16.9	75.8	7.3
33	$8b_2$	Cp(π)	−10.79	3.7	88.1	8.2
32	$6a_2$	Cp(π), Ti3d_{xy}, F(n)	−11.71	16.4	70.4	13.2
31	$11a_1$	Cp(π), Ti3d_{y^2}, F(σ)	−11.96	10.2	76.9	12.9
30	$8b_1$	Cp(π), F(n)	−13.21	0.3	80.7	19.0
29	$7b_2$	F(n), Cp(σ)	−13.45	0.1	30.4	69.5
28	$10a_1$	TiF(σ), Cp(σ)	−13.49	3.2	42.5	54.3
27	$5a_2$	F(n), Cp(σ)	−13.66	0.1	37.4	62.5
26	$6b_2$	Cp(σ), F(n)	−13.76	0.2	66.7	33.1
25	$9a_1$	F(n)	−13.80	4.3	4.7	91.0
24	$7b_1$	F(n), Cp(π)	−13.98	5.2	28.3	66.5
23	$4a_2$	Cp(σ)	−14.47	8.5	82.0	9.5
22	$8a_1$	Cp(σ), F(σ)	−14.54	11.1	60.0	28.9
21	$3a_2$	Cp(σ)	−14.64	9.1	76.8	14.1
20	$6b_1$	Cp(σ)	−14.83		97.5	2.5
19	$5b_2$	TiF(σ), Cp(σ)	−14.92	11.3	44.9	43.8

are $7b_2$ (−13.45 eV), $5a_2$ (−13.66 eV), $9a_1$ (−13.80 eV) and $7b_1$ (−13.98 eV); the calculated F contribution lies between 61 and 63%. A stronger coupling between the five-membered rings and the FTiF fragment is encountered in the two complex MOs of σ type ($10a_1$ at −13.49 eV and $5b_2$ at −14.92 eV). In the symmetric combination the ligand π contribution amounts to 42.5% and to 44.9% in the antisymmetric linear combination.

The INDO results for the chlorine complex *3* (Table III) indicate that the interaction between the two subunits is of more complicated nature. Various MOs are predicted where Cp π and chlorine contributions are of comparable magnitudes (class *B*). Typical representatives for this strong coupling scheme are the MOs $9b_1$, $7b_2$ and $8b_1$ where Cp π combinations interact with the chlorine lone-pair functions, or $10a_1$ with halide σ contributions. A less pronounced interaction is found in the case of $8b_2$, $6a_2$, $11a_1$ and $5a_2$ where one of the fragment contributions is predominant. The complex orbitals which are related to this coupling scheme span a

TABLE III. Valence Orbitals of Bis(cyclopentadienyl)titanumdichloride (*3*) According to an INDO Calculation. See Legend to Table I.

MO	Γ_i	MO-type	ϵ_i	% Ti	% Cp	% Cl
34	$9b_1$	Cl(n), Cp(π)	−8.66	4.2	46.3	49.5
33	$8b_2$	Cl(n), Cp(π)	−9.28	0.7	33.2	66.1
32	$6a_2$	Cl(n), Cp(π), Ti3d_{xy}	−9.38	5.6	25.2	69.2
31	$7b_2$	Cp(π), Cl(n)	−10.73	0.6	55.5	43.9
30	$11a_1$	Cl(n), Ti3d_{y^2}	−10.90	15.0	10.1	74.9
29	$10a_1$	TiCl(σ), Cp(π)	−11.04	2.8	40.1	57.1
28	$8b_1$	Cp(π), Cl(n), Ti3d_{xz}	−11.35	15.1	50.2	34.7
27	$9a_1$	Cp(π), Cl(n), Ti3$d_{x^2-z^2}$	−11.81	15.1	53.8	31.1
26	$5a_2$	Cp(π), Cl(n), Ti3d_{xy}	−12.02	9.8	63.1	27.1
25	$6b_2$	TiCl(σ), Ti3d_{yz}	−12.33	26.2	25.9	47.7
24	$7b_1$	Cp(σ)	−12.93	3.1	92.0	4.9
23	$5b_2$	Cp(σ)	−13.32	6.9	83.7	9.4
22	$4a_2$	Cp(σ)	−13.66	13.9	85.0	1.1
21	$8a_1$	Cp(σ)	−13.74	9.2	84.7	6.1
20	$3a_2$	Cp(σ)	−13.98	2.4	97.2	0.4

TABLE IV. Valence Orbitals of Bis(cyclopentadienyl)titanumdibromide (*4*) According to a CNDO Calculation. See legend to Table I.

MO	Γ_i	MO-type	ϵ_i	% Ti	% Cp	% Br
34	$9b_1$	Br(n), Cp(π)	−8.52	3.4	36.5	60.1
33	$8b_2$	Br(n), Cp(π)	−9.24	0.8	16.5	82.7
32	$6a_2$	Br(n), Cp(σ), Ti3d_{xy}	−9.42	7.4	17.3	75.3
31	$11a_1$	Br(n), Ti3d_{y^2}, Cp(π)	−9.87	19.5	9.1	71.4
30	$7b_2$	TiBr(σ), Ti3d_{yz}	−10.65	28.6	10.2	61.2
29	$10a_1$	TiBr(σ)	−11.23	3.4	4.3	92.3
28	$8b_1$	Cp(π), Ti3d_{xz}, Br(n)	−11.53	16.5	62.7	20.8
27	$6b_2$	Cp(π), Br(n), Ti3d_{yz}	−11.60	9.9	70.8	19.3
26	$9a_1$	Cp(π), Ti3$d_{x^2-z^2}$	−12.16	10.6	86.7	2.7
25	$5a_2$	Cp(π), Br(n), Ti3d_{xy}	−12.37	10.2	69.3	20.5
24	$7b_1$	Cp(σ)	−13.35	3.1	93.6	3.3
23	$5b_2$	Cp(σ)	−13.66	2.1	95.3	2.6
22	$8a_1$	Cp(σ)	−14.04	7.4	91.0	1.6
21	$4a_2$	Cp(σ)	−14.08	14.7	85.1	0.2
20	$3a_2$	Cp(σ)	−14.60	1.1	98.6	0.3

broad energy interval between −8.66 eV and −12.33 eV. The largest energy gap (1.35 eV) is predicted between the MOs $6a_2$ (−9.38 eV) and $7b_2$ at −10.73 eV. The MOs below the $6b_2$ linear combination correspond to Cp σ functions.

The CNDO results for the bromine complex (Table IV) indicate that *4* belongs to class *C*. The six highest occupied MOs are predominantly of the bromine type. $9b_1$, $8b_2$, $6a_2$ and $11a_1$, with one-electron energies of −8.52, −9.24, −9.42 and −9.87 eV, are bromine lone-pair combinations. The Br contribution in the corresponding orbital wave functions varies between 60.1% (*B/C* intermediate) and 83% (weak coupling limit *C*). In contrast to the previously analyzed interaction schemes a Cp σ/Br lone-pair coupling is encountered in $6a_2$. These four Br lone-

TABLE V. Net Charges in the Series *1–4* According to the Semiempirical INDO (*1, 2, 3*) and CNDO (*4*) Calculations.

Atom	*1*	*2*	*3*	*4*
Ti	−0.1202	0.8588	0.5017	0.2711
C_1	−0.1170	−0.0752	−0.1039	−0.1185
C_2/C_3	−0.0687	−0.0703	−0.0738	−0.0606
C_4/C_5	−0.0741	−0.1190	−0.1140	−0.1270
H_1	0.1158	0.1482	0.1284	0.1420
H_2/H_3	0.1093	0.1412	0.1223	0.1354
H_4/H_5	0.1008	0.1144	0.1056	0.1169
X = F, Cl, Br		−0.6350	−0.3555	−0.2883
C_{CO}	0.2807			
O_{CO}	−0.3542			

TABLE VI. Wiberg Bond Indices in the Ti Complexes *1–4* According to the INDO/CNDO Calculations.

Bond	*1*	*2*	*3*	*4*
TiX	0.773	0.543	0.820	0.818
X = C_{CO}, F, Cl, Br				
TiC_1	0.339	0.290	0.276	0.308
$TiC_{2/3}$	0.301	0.296	0.272	0.276
$TiC_{4/5}$	0.321	0.371	0.357	0.394
$C_1C_2 = C_1C_3$	1.233	1.311	1.303	1.267
$C_2C_4 = C_3C_5$	1.297	1.284	1.284	1.237
C_4C_5	1.236	1.196	1.209	1.191
CO	2.027			

pair orbitals are separated by 0.6 eV from MO $7b_2$, the antisymmetric BrTiBr σ combination with significant Ti $3d_{xy}$ amplitudes (29%). The symmetric $10a_1$ MO is predominantly localized at the Br centers (3.4% Ti admixtures). Next in energy the four MOs derived from e_1'/e_1'' are encountered: $8b_1$, $6b_2$, $9a_1$ and $5a_2$. The Br participation in these complex MOs is smaller than 21%.

The computational findings in the dihalide series *2* → *3* → *4* can be summarized as follows. In the F derivative the basis energies of the halide fragment orbitals are much lower than the Cp π orbital energies, leading to a weak coupling between both moieties (class *A*). Just the opposite is found in the Br complex (*C*) where the topmost orbitals are related to the BrTiBr fragment. The chlorine derivative lies between these extremes, the basis energies matching each other. The CNDO/INDO results are of course in line with the increasing electronegativity in the series F → Cl → Br (4.10 → 2.83 → 2.74 [32]), and with the variation of the first ionization potential of the halides (F = 17.42 eV, Cl = 13.01 eV, Br = 11.84 eV [33]).

The differences in the bonding capabilities in the series *1* to *4* are transparent, due to calculated atomic populations [34] and to Wiberg bond indices [35] (Tables V and VI). In the case of the dicarbonyl complex *1* it is found that the CO groups act as acceptors (metal-to-ligand charge transfer exceeds the ligand-to-metal transfer). In the halide series *2, 3* and *4* the decreasing electronegativity of X is manifested in the calculated net charges of Ti and of the halide, while the Cp population shows no remarkable modifications. The charge deficit at the 3d center is reduced from 0.8588 (*2*) to 0.2711 (*4*), while the halide net charge is changed from −0.6350 to −0.2883. The Ti halide coupling shows increasing covalent contributions in the series F → Cl → Br.

This is also shown in the Wiberg indices summarized in Table VI. The acceptor capability of the carbonyl groups in *1* is demonstrated by means of the small CO index (2.027) in comparison to the bond index of the uncomplexed ligand (2.450). Significant variations of the interaction strengths between Ti and the carbon centers of Cp are predicted. The TiC interaction is largest in the case of C_4/C_5 where Wiberg indices between 0.321 and 0.394 are calculated. The weakest coupling is found in the case of the carbon centers 2 and 3 where bond indices in an interval between 0.272 and 0.301 are diagnosed. It is the Ti $3d_{xz}$ AO that leads to the bond order modification. As summarized in Table VI this geometry-dependent TiCp coupling causes a significant bond alternacy in the cyclopentadienyl rings. The CC bond-order is smallest between those carbon centers where the metal Cp coupling is largest (C_4/C_5), and *vice versa*. The differences are most pronounced in the halide complexes *2* to *4*, while the alternacy properties of the dicarbonyl derivative are less marked.

The PE Spectra and the Green's Function Results

The PE spectrum of the dicarbonyl complex *1* shows two distinct maxima in the lower energy region below 12 eV [8]. Due to the intensity variation under He(I) and He(II) conditions it has been demonstrated that the first peak at 6.62 eV must be assigned to an ionization process from a MO with predominant Ti 3d character, while the broad band with a maximum at 9.15 eV has to be assigned to Cp ionization events. The third band system has maxima at 12.67, 13.19, 13.61 and 14.01 eV.

The calculated ionization energies by means of the Green's function approach are summarized in Table VII. In the expansion of the self-energy part, 17 hole-states and 7 particle-functions have been considered.

TABLE VII. Comparison between the Measured Vertical Ionization Potentials, $I_{v,j}^{exp}$, of *1* and the Calculated Ones, Assuming the Validity of Koopmans' Theorem, $I_{v,j}^{K}$, and Using the Inverse Dyson Equation ($I_{v,j}^{K} + \Sigma_{jj}^{(2)}(\omega_j)$, $I_{v,j}^{K} + \Sigma_{jj}^{eff}(\omega_j)$). All Values in eV.

Peak	Γ_j	$I_{v,j}^{K}$	$I_{v,j}^{K} + \Sigma_{jj}^{(2)}(\omega_j)$	$I_{v,j}^{K} + \Sigma_{jj}^{eff}(\omega_j)$	$I_{v,j}^{exp}$
1	$13a_1$	8.07	7.87	7.88	6.62
	$9b_1$	10.11	9.84	9.85	
	$9b_2$	10.45	10.17	10.18	
2	$6a_2$	11.08	10.72	10.74	9.15
	$12a_1$	11.36	11.00	11.02	
	$8b_1$	12.69	12.29	12.32	12.67
3	$8b_2$	13.10	12.72	12.74	13.19
	$11a_1$	13.36	13.01	13.03	
	$5a_2$	13.47	13.06	13.09	13.61
	$7b_1$	13.71	13.30	13.33	14.01

TABLE VIII. Comparison between the Measured and Calculated Ionization Potentials of *2*. See legend to Table VII.

Peak	Γ_j	$I_{v,j}^{K}$	$I_{v,j}^{K} + \Sigma_{jj}^{(2)}(\omega_j)$	$I_{v,j}^{K} + \Sigma_{jj}^{eff}(\omega_j)$	$I_{v,j}^{exp}$
1	$9b_1$	10.63	10.42	10.44	8.1
	$8b_2$	10.79	10.63	10.64	
2	$6a_2$	11.71	11.43	11.45	8.7
3	$11a_1$	11.96	11.72	11.74	9.4
4	$8b_1$	13.21	12.83	12.86	
	$7b_2$	13.45	12.95	12.97	
	$10a_1$	13.49	13.15	13.17	
	$5a_2$	13.66	13.13	13.17	
	$6b_2$	13.76	13.31	13.33	
	$9a_1$	13.80	13.25	13.28	13
	$7b_1$	13.98	13.47	13.49	max
	$8a_1$	14.54	14.18	14.20	
	$4a_2$	14.47	14.23	14.25	
	$3a_2$	14.64	14.31	14.32	
	$6b_1$	14.83	14.63	14.69	
	$5b_2$	14.92	14.68	14.69	

It is realized that the measured IPs are satisfactorily reproduced by the theoretical procedure. Band ① is assigned to the Ti $3d_{y^2}$ MO $13a_1$ while the second maximum corresponds to the four Cp π linear combinations $9b_1$, $9b_2$, $6a_2$ and $12a_1$. Although the calculated IPs are too large (by about 1 eV), the energy gap between the centers of gravity of bands ① and ② is predicted with high accuracy. The experimental separation amounts to 2.53 eV, theory predicts an energy gap of 2.57 eV. Additionally the calculated energy interval for the $9b_1$, $9b_2$, $6a_2$ and $12a_1$ ionizations (1.15 eV) is in good agreement with the measured band width of about 1.5 eV.

TABLE IX. Comparison between the Measured and Calculated Ionization Potentials of *3*. See Legend to Table VII.

Peak	Γ_j	$I^K_{v,j}$	$I^K_{v,j} + \Sigma^{(2)}_{jj}(\omega_j)$	$I^K_{v,j} + \Sigma^{eff}_{jj}(\omega_j)$	$I^{exp}_{v,j}$
	$9b_1$	8.66	8.38	8.40	8.50
1	$8b_2$	9.28	8.99	9.00	8.90
	$6a_2$	9.38	9.00	9.02	9.10
	$7b_2$	10.73	10.47	10.48	9.90
	$11a_1$	10.90	10.54	10.56	10.20
	$10a_1$	11.04	10.78	10.79	
2	$8b_1$	11.35	11.01	11.03	10.70
	$9a_1$	11.81	11.52	11.54	
	$5a_2$	12.02	11.69	11.71	11.00
	$6b_2$	12.33	11.98	12.00	
	$7b_1$	12.93	12.66	12.68	12.50
	$5b_2$	13.32	13.05	13.07	
3	$4a_2$	13.66	13.39	13.41	13.10
	$8a_1$	13.74	13.50	13.51	13.80
	$3a_2$	13.98	13.72	13.74	

The calculated ionization potentials indicate that Koopmans' theorem is a sufficient approximation for the calculation of the vertical IPs of *1*. Although MO $13a_1$ contains predominant Ti 3d amplitudes, only a Koopmans' defect of 0.19 eV is predicted. Comparable deviations from $I^K_{v,j}$ are also found for the ligand ionization processes.

Four band maxima were identified in the outer valence region in the PE spectrum of *2* [12]. Peaks ①, ② and ③ with approximate intensity ratios of 1:2:1 at 8.1, 8.7 and 9.4 eV belong to a common band system which is separated by about 4.5 eV from a broad system with an approximate maximum at 13 eV.

The calculated ionization potentials of *2* are collected in Table VIII. The zeros of the inverse Dyson equation have been obtained by taking into account 15 occupied MO's and 9 particle-states. The same dimensions for the self-energy operator have been employed in the case of the Cl and Br complexes. According to the INDO model peak ① has to be assigned to MO $9b_1$, peak ② to the MO-pair $8b_2/6a_2$ and the third maximum to $11a_1$. It is found that the measured peak separations and the calculated gaps are in good agreement: $\Delta I^{exp}_{1,2} = 0.6$ eV, $\Delta I^{exp}_{2,3} = 0.7$ eV, $\Delta I^{INDO}_{1,2} = 0.61$ eV, $\Delta I^{INDO}_{2,3} = 0.69$ eV. The intensity changes under He(II) conditions are in line with the given assignment. The ionization events of the fluorine MOs are predicted at higher energies and are found in the band system at 13 eV.

The calculated ionization energies in Table VIII indicate that Koopmans' defects are negligible; the calculated reorganization energies do not exceed 0.5 eV. While these findings are expected for the strongly delocalized Cp MOs, they are surprising in the case of the fluorine lone-pair combinations as remarkable reorganization effects have been calculated on different degrees of sophistication for small molecules with F atoms [23, 36, 37].

The PE spectrum of the chlorine complex *3* has the most complicated band shape in the series *1–4* [8, 10, 12]. In the outer valence region (below 14 eV) two different band systems are found that have a complex profile. Band ① has maxima at 8.5, 8.9 and 9.1 eV, the second system with maxima at 10.7 and 11.0 eV has two shoulders at the lower energy side with approximate origins at 9.9 and 10.2 eV. The third broad band system has maxima at 12.5, 13.1 and 13.8 eV. The variation of the cross sections under He(II) conditions indicates that the first two systems correspond to MOs with significant chlorine character, with a small Cl predominance in the second profile. Additionally it has been deduced that the low energy shoulder of this band is due to ionization events from MOs with significant Ti 3d amplitudes in the orbital wave function [12].

The INDO results in Table IX allow a straightforward rationalization of the IP sequence in *3*. The first three maxima are assigned to the MOs $9b_1$, $8b_2$ and $6a_2$ with calculated ionization energies of 8.40, 9.00 and 9.02 eV. The measured IPs differ only by about 0.1 eV (8.5, 8.9 and 9.1 eV) from the theoretical findings. The three MOs are the out-of-phase linear combinations between Cp π and chlorine

TABLE X. Comparison between the Measured and Calculated Ionization Potentials of *4*. See Legend to Table VII.

Peak	Γ_j	$I^K_{v,j}$	$I^K_{v,j} + \Sigma^{(2)}_{jj}(\omega_j)$	$I^K_{v,j} + \Sigma^{eff}_{jj}(\omega_j)$	$I^{exp}_{v,j}$
1	$9b_1$	8.52	7.99	8.03	8.8 max
	$8b_2$	9.24	8.56	8.61	
	$6a_2$	9.42	8.70	8.76	
	$11a_1$	9.87	9.46	9.51	
2	$7b_2$	10.65	10.16	10.23	9.60
	$10a_1$	11.23	10.38	10.43	
	$8b_1$	11.53	10.93	11.00	10.00
	$6b_2$	11.60	11.07	11.14	
	$5a_2$	12.37	11.66	11.74	10.50
	$9a_1$	12.16	11.74	11.81	
3	$7b_1$	13.35	12.76	12.82	12.30
	$5b_2$	13.66	13.00	13.07	
	$8a_1$	14.04	13.45	13.52	
	$4a_2$	14.08	13.45	13.53	13.70 max
	$3a_2$	14.60	14.14	14.18	

lone-pair orbitals. The stronger intensity reduction of the maxima at 8.9/9.1 eV under He(II) conditions is in line with the composition of the MOs, as summarized in Table III. The low energy shoulders at 9.9 and 10.2 eV are assigned to the orbitals $7b_2$, $11a_1$ and $10a_1$ which span an energy interval of 0.3 eV. It is the $11a_1$ MO that leads to the increase of the cross section under He(II) conditions, due to the significant Ti $3d_{y^2}$ participation. On the basis of the band intensities the maxima at 10.7 and 11.0 eV must always correspond to two ionization events. This assumption is supported by the INDO results, leading to the assignment of $8b_1/9a_1$ for the first component and to $5a_2/6b_2$ for the latter. As shown in Table III the calculated MO compositions are in line with the experimental intensity ratios [12]. The results of Table IX demonstrate that the sequence of the vertical ionization potentials is predicted with high accuracy. The deviations of the Green's function results from $I^K_{v,j}$ are not larger than 0.5 eV.

In the PE spectrum of the Br derivative two band systems are found in the lower energy region [12]. Band ① with a maximum at 8.8 eV and a half-width of about 0.8 eV must correspond to ionization events of MOs with predominant Br participation; the intensity is dramatically reduced under He(II) conditions. Band ② has three maxima at 9.6, 10.0 and 10.5 eV. A series of strongly overlapping bands with maxima at 12.3 and 13.7 eV is separated by about 2 eV from the second profile. The CNDO results on *4* are collected in Table X. It is seen here that the experimental ionization energies are well reproduced by the theoretical approach. The first system is assigned to the four Br lone-pair combinations $9b_1$, $8b_2$, $6a_2$ and $11a_1$, with a calculated center of gravity of 8.73 eV (exp.: 8.8 eV). The three components of the second band correspond to two ionization events for each maximum. The low energy component is due to the Br σ combinations $7b_2$ and $10a_1$, while the following peaks are assigned to the Cp π orbitals $8b_1/6b_2$ and $5a_2/9a_1$, respectively. As shown in Table X, $7b_2/10a_1$, $8b_1/6b_2$ and $5a_2/9a_1$ lead to three pairs where two functions always are nearly degenerate. The calculated energy gaps between the band maxima (0.75 eV and 0.71 eV, respectively) exceed only slightly the measured differences between the bands (0.4 and 0.5 eV). The calculated reorganization energies follow the theoretical results derived for the other Ti complexes, the PE spectrum of *4* can be assigned assuming the validity of Koopmans' theorem.

Conclusions

The PE spectra of bis(cyclopentadienyl)titanum derivatives have been investigated by means of a perturbational expansion based on the Green's function formalism within a semiempirical CNDO/INDO Hamiltonian. It has been demonstrated that the outer valence region in the PE spectra of the Ti dihalides

can be assigned on the basis of a classification for the coupling strength between the Cp e''_1/e'_1 fragment orbitals on one side and halide lone-pair and σ combinations on the other [12]. The dihalide complexes *2* and *4* belong to the weakly coupled species *A* and *C*, with small Cp halide mixing in the orbital wave functions. In *3* a stronger interaction between both moieties is encountered. The PE spectra and the MO properties of *3* and *4* differ partially from the behaviour of CpBeX metallocenes (X = Cl, Br) [38]. In both beryllium compounds the halide lone-pairs are on top of the degenerate Cp π combinations.

The calculated ionization potentials in the Tables VII–X clearly indicate that the deviations from Koopmans' theorem, $I^K_{v,j}$, are only of minor importance. In second order of perturbation the $I^K_{v,j}$ values are lowered by about 0.5 eV. The third order re-normalization contribution to the expansion of $\Sigma(\omega)$ is completely negligible. The absolute values of the renormalization are of the order of 0.05 eV. In the d^2 metallocene *1* a reorganization energy for the occupied 'Ti 3d' MO is predicted that is comparable with the observed Koopmans' defects of the delocalized ligand orbitals. On the other hand reorganization energies in Fe, Co and Ni complexes between 2.5 eV to 4.5 eV have been calculated within the present ZDO Hamiltonian [22, 39]. The reduction of the reorganization effects in the Ti complexes can be explained on the basis of recently-developed conceptions concerning the non-validity of Koopmans' theorem in transition metal compounds [22, 39]. In recent publications we have demonstrated that Koopmans' defects are largest in the case of strongly localized 3d AOs with small metal-ligand overlap. In this limit two-electron integrals with a pronounced short-range behaviour are calculated for the MOs with large metal 3d amplitudes. This potential leads to a predominance of the electronic relaxation in the increments of the self-energy part. With increasing delocalization of the 3d AOs, two-electron integrals are encountered, which show a more or less uniform long-range behaviour. In this case relaxation and correlation nearly compensate each other.

It is clear that the first situation is found in the extreme right of the 3d series leading to large Koopmans' defects in complexes containing Fe, Co, Ni or Cu as the transition metal center. Going to the left side of the first transition metal series (Sc, Ti, V) we come to a region where the one-center 3d Coulomb integrals are reduced while the covalent metal ligand coupling is enhanced, due to the more diffuse 3d orbitals. The reduction of the metal 3d two-electron integrals with simultaneous delocalization of the MOs with predominant 3d character leads to the situation where Koopmans' theorem is valid in molecules of the 3d series. To obtain some quantitative insight into the differences between a Ti complex and *e.g.* a Ni compound, we have collected experimental Coulomb integrals [41] for the 3d atoms and for C and O as ligand components in Table XI. It is seen that the Ti values are close to the one-center parameters of the ligands while the Ni Coulomb-integral (3d) is large in comparison with C and O two-electron elements.

TABLE XI. One-center Coulomb Integrals for C, O, Ti and Ni. All Values in eV [41].

	C	O	Ti	Ni
γ_{ss}	12.23	15.42	6.22	7.96
γ_{pp}	11.08	14.52	5.50	6.40
γ_{dd}			12.69	16.71

To extrapolate the theoretical findings for the Ti complexes it can be concluded that the non-validity of Koopmans' theorem is remarkably reduced and mitigated on the left of the 3d series; here $I^K_{v,j}$ is a reasonable approximation for vertical ionization energies in the outer valence region.

Acknowledgement

This work has been supported by the Stiftung Volkswagenwerk. The assistance of Mrs. I. Grimmer in the preparation of the manuscript is gratefully acknowledged.

References

1 P. C. Wailes, R. S. P. Coutts and H. Weigold, 'Organometallic Chemistry of Titanum, Zirconium and Hafnium', Academic Press, New York (1974).
2 G. Henrici-Olivé and S. Olivé, *Angew. Chem., 83,* 121 (1971);
Angew. Chem., *Int. Ed. Engl., 10,* 105 (1971).
3 C. Ballhausen and J. P. Dahl, *Acta Chem. Scand., 15,* 1333 (1961).
4 N. W. Alcock *J. Chem. Soc. A,* 2001 (1967).
5 J. C. Green, M. L. H. Green and C. K. Prout, *J. Chem. Soc. Chem. Commun.,* 421 (1972);
M. L. H. Green, *Pure Appl. Chem., 30,* 373 (1972).
6 H. H. Brintzinger and L. S. Bartell, *J. Am. Chem. Soc., 92,* 1105 (1970);
H. H. Britzinger, L. L. Lohr, Jr. and K. L. T. Wong, *ibid., 97,* 5146 (1975).
7 J. W. Lauher and R. Hoffmann, *J. Am. Chem. Soc., 98,* 1729 (1976).
8 I. Fragalá, E. Ciliberto and J. L. Thomas, *J. Organomet. Chem., 175,* C25 (1979).
9 G. Condorelli, I. Fragalá and A. Centineo, *J. Organomet. Chem., 87,* 311 (1975).
10 J. L. Petersen, D. L. Lichtenberger, R. F. Fenske and L. F. Dahl, *J. Am. Chem. Soc., 97,* 6434 (1975).

11 J. P. Clark and J. C. Green, *J. Less Common Met.*, 31 (1977).
12 C. Cauletti, J. P. Clark, J. C. Green, S. E. Jackson, I. L. Fragalá, E. Ciliberto and A. W. Coleman, *J. Electron Spectrosc., 18,* 61 (1980).
13 T. Koopmans, *Physica 1,* 104 (1934).
14 M. C. Böhm and R. Gleiter, *Theor. Chim. Acta, 59,* 127 (1981).
15 A. Veillard and J. Demuynck, in 'Modern Theoretical Chemistry', Vol. 4, ed. H. F. Schaefer, Plenum Press, New York (1977).
16 L. S. Cederbaum and W. Domcke, *Adv. Chem. Phys., 36,* 205 (1977).
17 F. J. Dyson, *Phys. Rev., 75,* 486 (1949).
18 D. J. Thouless, 'The Quantum Mechanics of Many Body Systems', Academic Press, New York (1961).
19 L. S. Cederbaum, *Theor. Chim. Acta, 31,* 239 (1973).
20 H. P. Kelly, *Phys. Rev., 131,* 684 (1963); *136B,* 896 (1964).
21 M. C. Böhm, *Inorg. Chem.*, submitted for publication; M. C. Böhm, *Chem. Phys.*, in press.
22 M. C. Böhm and R. Gleiter, *J. Comput. Chem., 3,* 140 (1982);
M. C. Böhm, R. Gleiter and W. Petz, *Inorg. Chim. Acta, 59,* 255 (1982);
M. C. Böhm, *Z. Naturforsch., 36a,* 1361 (1981);
M. C. Böhm, *J. Molec. Struct. (Theochem)*, in press;
M. C. Böhm, *Z. Physik. Chem.*, in press.
23 P. Lazzeratti and R. Zanasi, *Chem. Phys. Letters, 42,* 411 (1976);
B. J. Duke and M. P. S. Collins, *ibid., 54,* 304 (1978);
C. M. Liegener and U. Scherz, *Theor. Chim. Acta, 52,* 103 (1979).
24 G. Born, H. A. Kurtz and Y. Öhrn, *J. Chem. Phys., 68,* 24 (1978).
25 B. Kellerer, L. S. Cederbaum and G. Hohlneicher, *J. Electron Spectrosc., 3,* 107 (1974).
26 J. A. Pople and D. L. Beveridge, 'Approximate Molecular Orbital Theory', McGraw Hill, New York (1970).
27 J. L. Atwood, K. E. Stone, H. G. Alt, D. C. Hrncir and M. D. Rausch, *J. Organomet. Chem., 96,* C4 (1975).
28 B. R. Davis and I. Bernal, *J. Organomet. Chem., 30,* 75 (1971);
E. F. Epstein and I. Bernal, *Inorg. Chim. Acta, 7,* 211 (1973);
L. J. Petersen and L. F. Dahl, *J. Am. Chem. Soc., 97,* 6422 (1975).
29 S. Siegel, *Acta Cryst., 9,* 684 (1956).
30 P. Brand and J. Schmidt, *Z. anorg. Chem., 348,* 257 (1966).
31 P. S. Bagus, U. I. Wahlgren and J. Almlöf, *J. Chem. Phys., 64,* 2324 (1976);
J. H. Ammeter, H.-B. Bürgi, J. C. Thibeault and R. Hoffmann, *J. Am. Chem. Soc., 100,* 3686 (1978).
32 F. A. Cotton and G. Wilkinson, 'Anorganische Chemie', Verlag Chemie, Weinheim (1970).
33 C. E. Moore, *Atomic Energy Levels, Natl. Bureau Stand., 467,* (1949, 1952).
34 R. S. Mulliken, *J. Chem. Phys., 23,* 1833 (1955); *ibid., 23,* 2343 (1955).
35 K. B. Wiberg, *Tetrahedron, 24,* 1083 (1968).
36 L. S. Cederbaum, G. Hohlneicher and W. v. Niessen, *Mol. Phys., 26,* 1405 (1973);
L. S. Cederbaum, *Chem. Phys. Letters, 25,* 562 (1974).
37 D. P. Chong, F. G. Herring and D. McWilliams, *J. Chem. Phys., 61,* 78, 3587 (1974).
38 M. C. Böhm, R. Gleiter, G. L. Morgan, J. Lusztyk and K. B. Starowieyski, *J. Organomet. Chem., 194,* 257 (1980).
39 M. C. Böhm, in preparation.
40 J. S. Griffith, 'The Theory of Transition-Metal Ions', Cambridge University Press (1971);
M. Gerloch and R. C. Slade, 'Ligand-field Parameters', Cambridge University Press (1973).
41 L. Oleari, L. Di Sipio and G. De Michelis, *Mol. Phys., 10,* 97 (1966);
L. Di Sipio, E. Tondello, G. De Michelis and L. Oleari, *Chem. Phys. Letters, 11,* 287 (1971).